

# The nature of assembly bias - II. Halo spin

Ivan Lacerna<sup>1,2</sup> and Nelson Padilla<sup>1,3</sup>

<sup>1</sup>*Departamento de Astronomía y Astrofísica, Pontificia Universidad Católica de Chile, V. Mackenna 4860, Santiago, Chile*

<sup>2</sup>*Instituto de Astronomía, Universidad Nacional Autónoma de México, A. P. 70-264, 04510, México, D.F., México*

<sup>3</sup>*Centro de Astro-Ingeniería, Pontificia Universidad Católica de Chile, V. Mackenna 4860, Santiago, Chile*

## ABSTRACT

We study an assembly-type bias parametrized by the dimensionless spin parameter that affects massive structures. In numerical simulations higher spin haloes are more strongly clustered than lower spin haloes of equal mass. We detect a difference of over a 30 per cent in the clustering strength for dark matter haloes of  $10^{13} - 10^{14} h^{-1} M_{\odot}$ , which is similar to the result of Bett et al. We explore whether the dependence of clustering strength on halo spin is removed if we apply the redefinition of overdensity peak height proposed by Lacerna & Padilla (Paper I) obtained using assembly ages. We find that this is not the case due to two reasons. Firstly, only a few objects of low-virial mass are moved into the mass range where the spin introduces an assembly bias after using this redefinition. Secondly, this formalism does not alter the mass of massive objects. In other words, the sample of haloes with redefined mass  $M$  in the high-mass regime is practically the same as before the redefinition of peak height, and thus the clustering behaviour is the same. We then repeat the process of finding the redefined peak height of Paper I but using the spin. In this case, the new masses show no spin-related assembly bias but they introduce a previously absent assembly bias with respect to relative age. From this result, we conclude that the assembly-type bias with respect to the halo spin has a different origin than with respect to assembly age. The former may be due to the material from filaments, which is accreted by massive haloes, that is enhanced in high-density environments, thus causing more extreme spin values without significantly changing the formation age of the halo. In addition, the estimates of the mass of collapsed structures in numerical simulations could be lower than the true mass, even in cluster-size haloes. High-mass objects may correspond, in some cases, to a different peak height than that suggested by their virial mass, providing a possible explanation for the assembly bias with respect to spin.

**Key words:** cosmology: theory - dark matter - large-scale structure of Universe.

## 1 INTRODUCTION

The new generation of numerical simulations of high resolution have shown that the large-scale clustering of haloes of a given mass varies significantly with their assembly history (Gao & White 2007). This effect, which is not expected from the extended Press–Schechter theory (Bond et al. 1991), was termed ‘assembly bias’, and is found when measuring the amplitude of clustering as a function of halo properties such as formation time and halo spin at fixed halo mass.

In the first paper of this series, we presented a new approach to estimate the overdensity peak height with the aim to understand the assembly bias effect (Lacerna & Padilla 2011, hereafter Paper I). The method consisted in redefining the overdensity that characterizes each object using the information of its virial mass and relative age. This new

definition is proposed as a better alternative than the virial mass as a proxy for equivalent peak height.

In this letter we will investigate the prevalence of the assembly bias with the proposed redefinition of an overdensity peak height of Paper I using the dimensionless spin parameter. Works by Bett et al. (2007, hereafter B07) and Faltenbacher & White (2010) have detected an assembly-type bias in massive dark matter (sub)haloes using this property. They found that higher spin objects are more strongly clustered than lower spin objects of equal mass.

The outline of this work is as follows. Section 2 describes the data, and the dimensionless spin parameter is defined in Section 3. The detection of the assembly bias in our simulation using halo spin is shown in Section 4, and Section 5 shows the results using the overdensity peak height proxy. The discussion and conclusions are presented in Section 6.

## 2 DATA

The numerical simulation we use in this letter is called **STAND**, and consists of a periodic box of  $150 h^{-1}$  Mpc on a side. It contains  $640^3$  dark matter particles with a mass resolution of  $\sim 10^9 h^{-1} M_\odot$ . The cosmology used in this simulation is  $\Omega_m = 0.28$  (with a baryon fraction of 0.164),  $\Omega_\Lambda = 0.72$ ,  $\sigma_8 = 0.81$ ,  $h = 0.7$ , and spectral index  $n_s = 0.96$ . The chosen value of  $\sigma_8$  is in good agreement with recent results of WMAP (Komatsu et al. 2011). The simulation is run from redshift  $z = 73.5$  using the initial conditions of **GRAFIC2** (Bertschinger 2001) and the public version of the **GADGET-2** code (Springel 2005).

In 99 snapshots of the simulation, dark matter haloes are identified as structures that contain at least 10 particles using a friends-of-friends (FOF) algorithm (Davis et al. 1985). Another algorithm (SUBFIND; Springel et al. 2001) is applied to these groups in order to find substructures with at least 10 particles.

The catalogues of haloes and subhaloes are used to construct merger histories, over which the SAG2 model by Lagos, Cora, & Padilla (2008; see also Lagos, Padilla, & Cora 2009) is run to produce a galaxy population. In this letter, we only use the central galaxy of the most massive subhalo within a FOF halo.

## 3 DIMENSIONLESS SPIN PARAMETER

The dimensionless spin parameter  $\lambda$  is typically defined as (Peebles 1971)

$$\lambda = \frac{J|E|^{1/2}}{GM_h^{5/2}}, \quad (1)$$

where  $J$  is the magnitude of the angular momentum vector,  $E$  is the total energy,  $G$  is the gravitational constant, and  $M_h$  is the mass of the FOF halo defined by the number of dark matter particles,  $N_p$ . The angular momentum is

$$\mathbf{J} = \frac{M_h}{N_p} \sum_{i=1}^{N_p} \mathbf{r}_i \times \mathbf{v}_i \quad (2)$$

where  $\mathbf{r}_i$  and  $\mathbf{v}_i$  are the position and velocity vectors of particle  $i$  relative to the halo centre of mass, respectively. Furthermore, the total energy of the system is given by  $E = T + U$ , where  $T$  corresponds to the kinetic energy and  $U$  to the potential energy.

We select haloes with number of particles  $N_p \geq 300$  because they have reliable estimates of this parameter (B07). The number of selected objects using this condition is 31,449 haloes, which corresponds to four per cent of the total sample. As noted by B07, there is an important scatter at higher spins even for  $N_p \geq 300$  due to small objects with high velocity dispersions, caused by the proximity of more-massive haloes. This velocity contamination increases the kinetic energy of small haloes,  $T$ , resulting in larger values of spin. To overcome this problem, they suggested the quasi-equilibrium criterion to remove anomalous spin haloes. This is a cut of the instantaneous virial ratio of halo energies  $2T/U + 1$ . Typically, a virialized object has a value around zero, and a gravitationally bound object has value  $\geq -1$ . We select the haloes according to

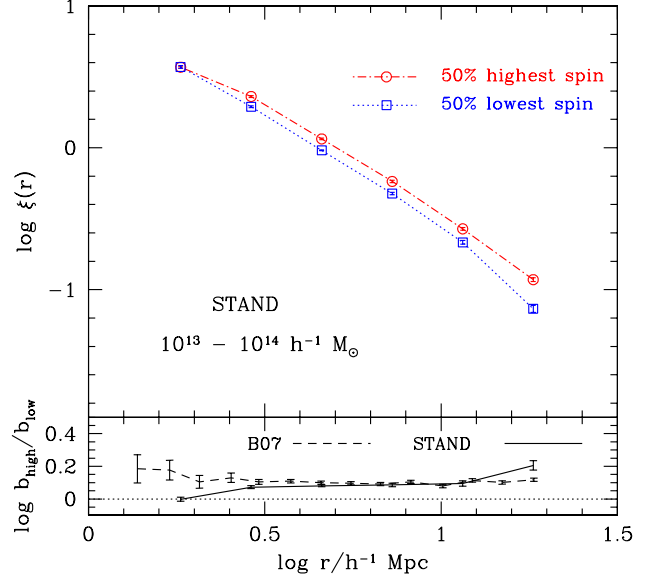


**Figure 1.** Main panel (top): two-point cross-correlation function for haloes in the **STAND** simulation. The result for the 50 per cent highest spin haloes is represented as dot-dashed red lines, whereas that for the 50 per cent lowest spin haloes appears as dotted blue lines. Error bars were calculated using the jackknife method. Lower panel (bottom): ratio between the bias of high and low spin objects in the **STAND** simulation (solid lines) and in B07 (dashed lines). At large scales,  $r > 3 h^{-1}$  Mpc, both simulations show a higher clustering for high spin haloes with respect to low spin ones with a similar signal, which is over 30 per cent.

$$-Q \leq \frac{2T}{U} + 1 \leq Q, \quad (3)$$

where the limit value is  $Q = 0.5$  (B07). This allows us to remove objects with anomalous spins. The final sample contains 29,633 haloes.

Although the spin  $\lambda$  has little dependence on mass, if any, we define the relative spin parameter, in analogy to the relative age parameter  $\delta_t$  of Paper I, as

$$\delta_{\lambda_i} = \frac{\lambda_i - \langle \lambda(M) \rangle}{\sigma_\lambda(M)}, \quad (4)$$

where, for the  $i$  th object,  $\lambda_i$  is its dimensionless spin,  $\langle \lambda(M) \rangle$  is the median spin as a function of FOF host halo mass  $M$ , and  $\sigma_\lambda(M)$  is the dispersion around the median. Then, positive values of  $\delta_\lambda$  correspond to high spin objects, whereas negative values of  $\delta_\lambda$  are related to low spin objects.

## 4 ASSEMBLY BIAS USING HALO SPIN

In this section, we will use the two-point correlation function to test whether dark matter (DM) haloes from the **STAND** simulation show an assembly-type bias with the halo spin.

Figure 1 shows the two-point cross-correlation function

of DM haloes of equal mass but different relative spin parameter given by equation (4). The centres to perform  $\xi(r)$  are haloes selected in the mass range  $10^{13} - 10^{14} h^{-1} M_{\odot}$ , and the tracers are all the haloes in the final sample (see Section 3) in order to obtain a better signal-to-noise. The 50 per cent high spin haloes are more strongly clustered at large scales than the 50 per cent low spin haloes, thus showing an assembly-type bias. The lower panel shows the ratio between the bias of high and low spin objects in the STAND simulation (solid line). This ratio is calculated as

$$\frac{b_{H,high\lambda}}{b_{H,low\lambda}} = \frac{\xi_{HH',high\lambda}}{\xi_{HH',low\lambda}}, \quad (5)$$

where the subscript  $H$  refers to centres and  $H'$  to tracers. We compare to the autocorrelation function results of B07 shown as a dashed line in the lower panel. In this case, the ratio between the bias of 50 per cent high and 50 per cent low spin objects is calculated as

$$\frac{b_{H,high\lambda}}{b_{H,low\lambda}} = \sqrt{\frac{\xi_{HH,high\lambda}}{\xi_{HH,low\lambda}}}. \quad (6)$$

As can be seen from the lower panel, at scales  $r > 3 h^{-1} \text{Mpc}$ , both simulations show a higher clustering for high spin haloes with respect to the low spin ones (over a 30 per cent difference) with a comparable signal.

## 5 OVERDENSITY PEAK HEIGHT PROXY

In Paper I, we presented an approach to trace the assembly bias effect. This consisted in measuring the total mass inside spheres of different radii around semi-analytic galaxies, which in some cases returned larger values than the virial mass of the host dark matter halo, using two free parameters to introduce a dependence of this radius on mass and age. This model defined a new overdensity peak height for which the large-scale clustering of objects of a given mass did not depend on the age. The parametrization helps to characterize the environment and to understand what is behind the assembly bias (see Paper I for more details).

### 5.1 Parametrization using the relative age

We will first use the same approach of Paper I in order to find the best-fitting parameters so that  $\xi(r)$  does not show a dependence of the large-scale clustering on age. We will then use the parametrization to study whether the dependence on spin is still present.

For this purpose, we match up the position of central semi-analytic galaxies with the position of the selected haloes in order to estimate the relative age of these haloes using

$$\delta_{t_i} = \frac{t_i - \langle t(M) \rangle}{\sigma_t(M)}, \quad (7)$$

where, for the  $i$  th galaxy,  $t_i$  is its mass-weighted stellar age,  $\langle t(M) \rangle$  is the median stellar age as a function of host halo mass  $M$ , and  $\sigma_t(M)$  the dispersion around the median in units of time. The procedure is successful in the 99 per cent of the cases, so that the final sample contains 29,376 haloes for which the results shown in Figure 1 are the same. In

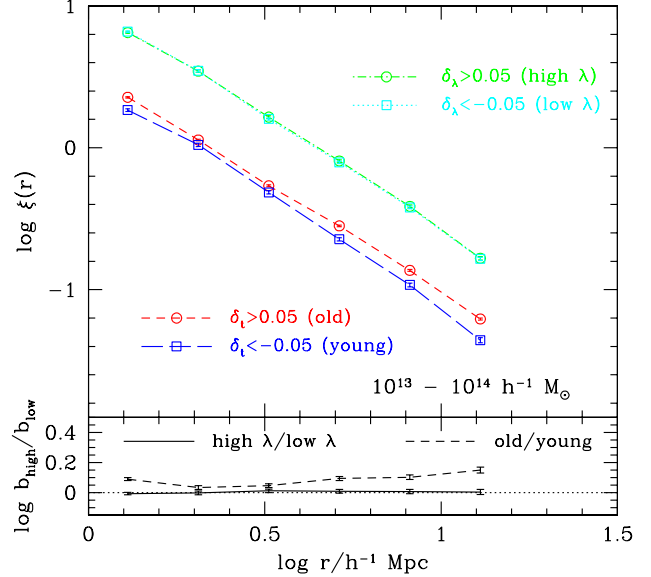


**Figure 2.** Two-point cross-correlation function for haloes of equal redefined mass but different spin and different age from the STAND simulation. The best-fitting parameters are  $a = -0.36$  and  $b = -1.52$ , where the reduced  $\chi^2$  statistics is performed using the spin (Section 5.2). Error bars are calculated using the jackknife method. The high-spin population is represented as a dot-dashed green line, whereas the low-spin population is represented as a dotted cyan line. The old population is represented as a short-dashed red line, whereas the young one appears as a long-dashed blue line. For clarity, these two lines are moved -0.5 dex in the vertical direction. Lower panel: ratio between the bias of high-spin and low-spin objects (solid line) and between the bias of old and young objects (dashed line). The dotted line represents the ratio equal to unity.

the other 257 objects, which include some massive haloes of  $10^{14.5} h^{-1} M_{\odot}$ , the position of the central galaxy is very far away from the central position of the halo. We use the condition  $d \leq 250 h^{-1} \text{kpc}$ , where  $d$  is the distance between the position of the central galaxy and centre of mass of the DM halo. We do not assign the age of the central galaxy to its host halo at distances beyond this limit. Again, these ‘failures’ correspond to just one per cent of the haloes. The resulting stellar age as a function of halo mass is qualitatively similar to that shown in Paper I. On average, more massive objects have older stellar ages.

We redefine the overdensity peak height within spheres around haloes of mass  $M_h$ , for which the radius of a sphere (in  $h^{-1} \text{Mpc}$  units) is parametrized as

$$r = a \delta_t + b \log \left( \frac{M_h}{M_{nl}} \right), \quad (8)$$

where  $M_{nl}$  is the non-linear mass defined by Seljak & Warren (2004),  $\log(M_{nl}/h^{-1} M_{\odot}) = 13.24$  for the choice of cosmological parameters in the STAND simulation. The free parameters are  $a$  and  $b$ . The new peak height proxy will be the mass  $M$  enclosed within this radius. It is assumed that if  $r$  is smaller than the virial radius or if  $M$  is smaller than the halo mass, then  $M = M_h$ . The  $\chi^2$  statistics to find the

best-fitting set of free parameters is defined as

$$\chi^2_{\xi(r)} = \frac{1}{N} \sum_i \left( \frac{1}{n_{dof}} \sum_r \frac{[\xi_{high}(r) - \xi_{low}(r)]^2}{\sigma^2} \right)_i, \quad (9)$$

where  $\xi_{high}(r)$  and  $\xi_{low}(r)$  is the result for old and young haloes, respectively. The error is  $\sigma^2 = \sigma_{\xi_{high}}^2 + \sigma_{\xi_{low}}^2$ , where the first term is the jackknife error for  $\xi_{high}(r)$  and the second for  $\xi_{low}(r)$ . The symbol  $n_{dof}$  denotes the number of degrees of freedom ( $n_{dof} = 6$ ). This statistics is calculated within  $1 \leq r/h^{-1} \text{ Mpc} \leq 13$  over three mass bins (the first, second and third terciles of the mass distribution), i.e.  $N = 3$ .

The best-fitting values are  $a = 0.08$  and  $b = -0.37$ . As in Paper I, the assembly bias with respect to age is not present at large scales after performing this procedure. However, the differences in the clustering strength of haloes of equal high mass but different spin will still be present because just one halo of low virial mass is considered in this high-mass range after using the parametrization. Also, as mentioned in Paper I, this formalism does not alter the mass of objects with high mass. Therefore, the sample of haloes with masses between  $10^{13}$  and  $10^{14} h^{-1} M_{\odot}$  is practically the same, thus showing the same clustering behaviour as before.

## 5.2 Parametrization using spin

To trace the assembly bias with the dimensionless spin parameter, we use the reduced  $\chi^2$  statistics defined in eq. (9), but in this case  $\xi_{high}(r)$  and  $\xi_{low}(r)$  correspond to the cross-correlation function for high-spin and low-spin haloes, respectively. This statistics is calculated within  $1 \leq r/h^{-1} \text{ Mpc} \leq 13$  over two mass bins,  $10^{12} - 10^{13} h^{-1} M_{\odot}$  and  $10^{13} - 10^{14} h^{-1} M_{\odot}$ , i.e.  $N = 2$ .

The best-fitting values are  $a = -0.36$  and  $b = -1.52$ . After applying the redefinition of mass there is no difference in the clustering amplitude for massive haloes of high and low spin at large scales, as can be seen in Figure 2. In contrast, it can be seen in the same figure an artificial assembly bias with respect to age using this set of parameters. Note that the assembly bias for objects of equal mass but different age affects low-mass haloes (Gao, Springel & White 2005). Therefore, the formalism applied to the assembly-type bias with the dimensionless spin parameter  $\lambda$  is not related with the successful overdensity peak height defined in Paper I. For example, Figure 3 shows that the mean radius for haloes of intermediate mass is  $10r_{vir}$  (solid line), which is larger compared to  $1 - 4r_{vir}$  described in Paper I. Furthermore, a few very massive objects changed their masses (dashed line), an aspect that was not found in the redefinition of the overdensity peak height that explains the assembly bias using the age.

## 6 DISCUSSION AND CONCLUSIONS

Perhaps the assembly-type bias found in massive objects of equal mass but different spin values is related with the massive neighbours responsible for the truncation of the growth of smaller objects reported in Paper I. High mass haloes reach virial masses according to theoretical expectations, but those in high density environment accrete an important fraction of material from filaments (Hahn et al. 2009).

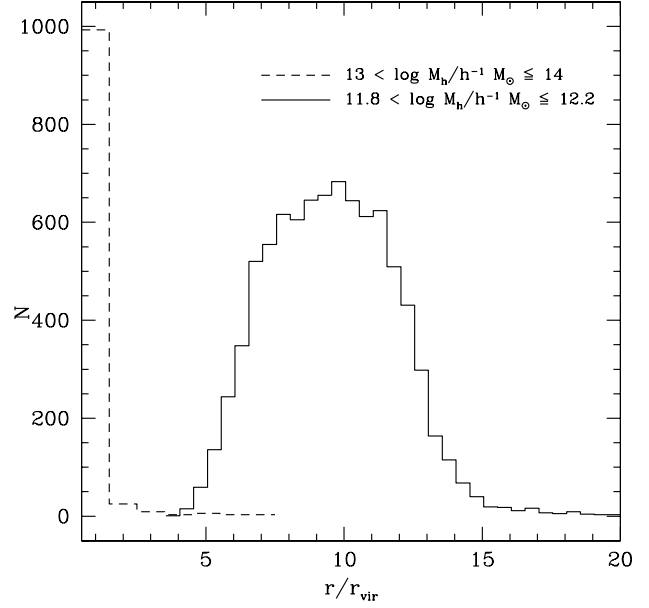


**Figure 3.** Distribution of radius  $r$  of eq. (8) in units of virial radius  $r_{vir}$  for two ranges of halo mass  $M_h$  from the STAND simulation for the parametrization using spin (see Section 5.2). Haloes of intermediate mass (solid line) have mean radius of  $10r_{vir}$ , which is larger compared to  $1 - 4r_{vir}$  described in Paper I. Also, a few very massive objects (dashed line) have  $r > r_{vir}$ , in contrast to the redefinition of the overdensity peak height that explains the assembly bias using the age.

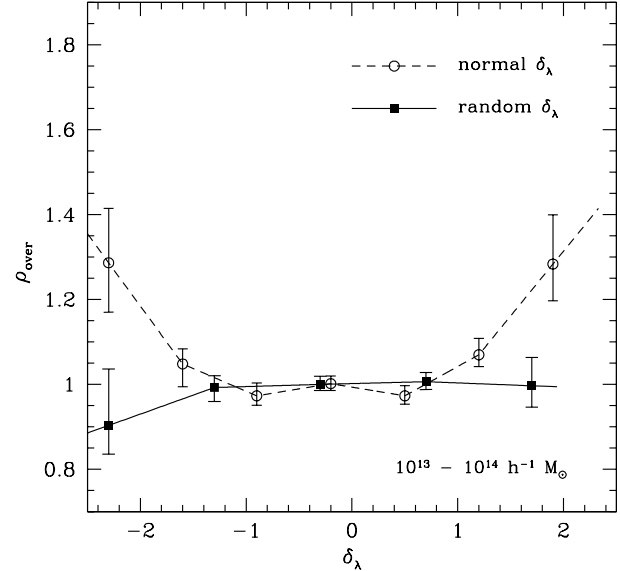


**Figure 4.** Median overdensity as a function of relative spin parameter,  $\delta_{\lambda}$ , for massive haloes in the STAND simulation. Open circles (dashed line) correspond to normal  $\delta_{\lambda}$  values. Filled squares (solid line) correspond to randomly swapped  $\delta_{\lambda}$  values (see details in Section 6). The error bars correspond to the error of the median in both cases.

This highly collimated material could cause changes in the angular momentum of these haloes affecting their spin. On the other hand, low-mass objects of equal mass do not show important differences in clustering when they are split in samples of high and low spin  $\lambda$  showing a lack of dependence with the environment (B07). However, we have already mentioned that small haloes in the vicinities of massive neighbours are discarded in this kind of analysis since they suffer velocity contamination that increases their kinetic energy, thus increasing their spin values. Probably, massive haloes fed by material in the region of a truncated smaller halo suffer a similar contamination that alters their spins.

The environmental dependence of massive ( $13 \leq \log(M_h/h^{-1} M_\odot) \leq 14$ ) haloes is shown in Figure 4. This dependence is estimated as the median overdensity ( $\rho_{over}$ ) as a function of relative spin parameter,  $\delta_\lambda$ . The density is calculated using all the available haloes in the simulation. We then estimate the overdensity with respect to the median. As can be seen, a smooth dependence with environment is found for low-spin and high-spin objects of equal mass (dashed line). It is worth to mention that extreme values of spin are represented by higher or lower values of  $\delta_\lambda$ . Therefore, it is plausible that the assembly-type bias found by using the spin parameter is due to a density enhancement that affects the spin values of massive objects.

In order to remove this dependence with environment, the relative spin parameter  $\delta_\lambda$  is randomly swapped among haloes in mass ranges of 0.1 dex (see the resulting solid line in Figure 4), without altering their positions. After performing this procedure, the halo clustering dependence on spin is practically absent, as can be seen in Figure 5. The average difference in clustering strength between the fifty per cent highest spin haloes and the fifty per cent lowest spin haloes is smaller than a 10 per cent, showing that the density enhancement can affect the properties of massive objects such as the spin.

Therefore, in the context of the peak formalism, the large amount of material from filaments from the cosmic web that a massive halo accretes in high density regions might also affect its final mass, thus introducing a spurious apparent change in the bias. Furthermore, tools used to identify objects in numerical simulations, such as FOF or SUBFIND, often define structures located very close to a massive object as a separated identity. Anderhalden & Diemand (2011) developed a formalism to identify lost particles, where many small structures actually belong to a neighbour massive object. As a consequence, the mass estimation of structures in numerical simulations, even in cluster-size haloes, could be lower than the actual mass. It is remarkable that the age of massive objects is not strongly affected by this discrepancy in mass; however this phenomenon is important in properties that are directly related with groups of DM particles in high density environments such as the spin, which can produce an assembly bias effect.

We would like to thank Darren Croton, Gaspar Galaz, Leopoldo Infante and the anonymous referee for comments and discussions. We acknowledge support from FONDAP “Centro de Astrofísica” 15010003, BASAL-CATA, Fondecyt grant No. 1110328, CONICYT, and MECESUP. IL acknowledges support from DGAPA-UNAM. The calculations

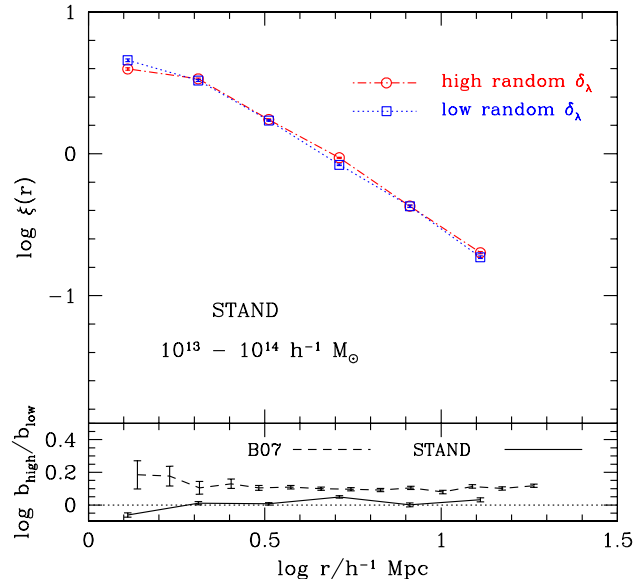


**Figure 5.**  $\xi(r)$  for massive haloes from the STAND simulation. Relative spin parameter  $\delta_\lambda$  is randomly swapped among haloes in mass ranges of 0.1 dex. The result for 50 per cent highest spin haloes is represented as dot-dashed red lines, whereas that for 50 per cent lowest spin haloes appears as dotted blue lines. Error bars are calculated using the jackknife method. Lower box: ratio between the bias of high and low spin objects in the STAND simulation (solid line) and in B07 (dashed line). The average difference in clustering amplitude is smaller than a 10 per cent when halo spins of the STAND simulation are randomly distributed.

for this work were performed using the Geryon cluster at the Centre for Astro-Engineering at UC.

## REFERENCES

- Anderhalden D., Diemand J., 2011, MNRAS, 414, 3166
- Bertschinger E., 2001, ApJS, 137, 1
- Bett P., et al., 2007, MNRAS, 376, 215
- Bond J. R., Cole S., Efstathiou G., Kaiser N., 1991, ApJ, 379, 440
- Davis M., Efstathiou G., Frenk C., White S. D. M., 1985, ApJ, 292, 371
- Faltenbacher A., White S. D. M., 2010, ApJ, 708, 469
- Gao L., Springel V., White S. D. M., 2005, MNRAS, 363, 66
- Gao L., White S. D. M., 2007, MNRAS, 377, L5
- Hahn O., Porciani C., Dekel A., Carollo C. M., 2009, MNRAS, 398, 1742
- Komatsu E., et al., 2011, ApJS, 192, 18
- Lacerna I., Padilla N., 2011, MNRAS, 412, 1283 (Paper I)
- Lagos C., Cora S. A., Padilla N., 2008, MNRAS, 388, 587
- Lagos C., Padilla N., Cora S., 2009, MNRAS, 395, 625
- Peebles P. J. E. 1971, A&A, 11, 377
- Seljak U., Warren M. S., 2004, MNRAS, 355, 129
- Springel V., 2005, MNRAS, 364, 1105
- Springel V., White S. D. M., Tormen G., Kauffmann G., 2001, MNRAS, 328, 726